Available online at www.sciencedirect.com
SCIENCE DIRECT®
Journal of Power Sources 119–121 (2003) 929–933
JOURNAL OF POWER SOURCES
www.elsevier.com/locate/jpowsour

Influence of capacity fading on commercial lithium-ion battery impedance

T. Osaka[a,*], S. Nakade[b], M. Rajamäki[c], T. Momma[a,d]

[a]*Graduate School of Science and Engineering, Kagawa Memorial Laboratory for Material Science and Technology, Waseda University, Shinjyuku, Tokyo 169-8555, Japan*
[b]*Nokia Research Center, Nokia-Japan Co. Ltd., 2-13-5 Nagata-cho, Tokyo 100-0014, Japan*
[c]*Nokia Mobile Phones, Nokia-Japan Co. Ltd., 2-13-5 Nagata-cho, Tokyo 100-0014, Japan*
[d]*CREST, JST, 4-1-8, Honcho, Kawaguchi, Saitama 332-0012, Japan*

Abstract

The impedance spectrum of prismatic commercial Li-ion batteries is measured at various states of charge before and after the charge–discharge cycles and storage. The measured impedance is interpreted with a previously proposed equivalent circuit made up of anode and cathode in which the cathode component is composed of two particle size factors. The values corresponding to the characteristics of both electrodes are obtained by a fitting technique. The obtained values suggest that the capacity fade of the Li-ion battery due to the cycles is mainly caused by the increase of interfacial resistance of the cathode and a decrease in the anode capacity. These results suggest the validity of the equivalent circuit to interpret the causes of capacity fade.

Keywords: Li-ion battery; Impedance; Capacity fade

1. Introduction

Lithium-ion rechargeable batteries have been widely adopted in portable electronic devices due to their high energy density. It is desirable that the capacity of the battery retains the initial capacity with usage time. However, the capacity of current Li-ion batteries decreases with the number of charge–discharge cycles and with the storage time. Since the batteries are used with tens to hundreds of charge–discharge cycles, improving the cycle performance and lifetime of Li-ion batteries remains an important issue.

To understand the mechanism of capacity fading, efforts have been made by various groups [1]. Most current Li-ion batteries consist a $LiCoO_2$ cathode and a carbon anode. It has been known that electrolytes decompose on the surface of the electrode and form surface layers during the charge–discharge cycles [1,2]. This reaction increases the interfacial resistance and hence decreases the capacity. The capacity fading also occurs by active material dissolution and phase changes of the materials. To study these phenomena for commercial batteries, the battery cell is typically opened, which is inconvenient to track the continuous changes with the cycle and storage.

Electrochemical impedance spectroscopy has been applied as one investigation method to commercial Li-ion batteries [3–7]. Previous studies have shown that measured impedance spectra consisted of a small semicircle at high frequency, large semicircle at middle frequency, and diffusion related impedance at low frequency. The measurements preformed with and without a reference electrode showed that the large circle at middle frequency was mainly attributed to the cathode [3–5]. The small semicircle of high frequency was proved to be attributed to the anode. The influences of the battery temperatures [4,5] and charge–discharge cycles [3,5] were also studied by analyzing mainly the two semicircles on the impedance spectra. It was finally concluded that the cathode was the main cause of impedance increase and consequently the reason for capacity fade. However, few were concerned about the impedance, including at very low frequency.

Previously, Momma et al. proposed an equivalent circuit for commercial Li-ion batteries for a wide range of impedance spectra [8,9]. The impedance of Panasonic batteries was measured without a reference electrode, and the fitting results showed that this was a convenient method to study the capacity fade with two electrode measurements [10].

In this study, the equivalent circuit was applied to different commercial batteries from the previous ones. The state of the batteries was analyzed to demonstrate how the

* Corresponding author. Tel.: +81-3-5286-3202; fax: +81-3-3205-2074.
E-mail address: osakatet@mn.waseda.ac.jp (T. Osaka).

0378-7753/03/$ – see front matter
doi:10.1016/S0378-7753(03)00233-7

capacity fade of the batteries can be assessed in a non-destructive method.

2. Experimental

Sample Li-ion batteries were chosen from commercially available batteries. The shape was prismatic with a nominal capacity of 680 mAh. The impedance of the batteries was measured with a potentiostat (Hokuto Denko, HA501) and a frequency response analyzer (NF Corporation, 5720) with an ac signal amplitude of 10 mV. Potential step chronoamperometry was also performed with the potentiostat, and the current transients were recorded on a PC through an A/D converter. For these measurements, the counter electrode was also used as a reference electrode. The batteries were charged and discharged with a constant current–constant voltage (CC–CV) protocol between 2.75 and 4.1 V with a 2 C rate. Another set of batteries was stored in a 50 °C environment for 20 days. All measurements were performed at room temperature.

Measured impedances were fitted with the equivalent circuit shown in Fig. 1. The descriptions of this circuit are written in detail elsewhere [9]. In short, the circuit was designed with several assumptions and considerations taking into account the structure of commercial batteries. Impedance of the electrode–electrolyte interface has been considered with surface film(s) and a double layer. Here, each layer is probably equivalent with a resistance and capacitance in parallel. Hence, each electrode has at least two capacitance–resistance components. Since the measurements were performed without a reference electrode, it would be difficult to separate each contribution by fitting if the measured impedance has only two distinct semicircles. Here, it is assumed that one couple of resistance and capacitance describes each electrode adequately. This assumption should be valid if the impedance of one electrode dominates one semicircle, which may be the case [3,4]. The two Warburg impedances in parallel were designed with a presumption that the electrode consisted of two different sizes of particles, resulting in two different diffusion paths. The reason for the mixture might be found in the fact that the mixture of different size particles for the cathode will increase the capacity with a decrease of resistance [11]. In this report, the contribution of the two Warburg impedances to total impedance was assumed to be one to one. The Warburg impedance can be expressed by:

$$Z = \frac{R}{\sqrt{iwT}} \mathrm{Coth}(\sqrt{iwT}) \quad (1)$$

where w is frequency, $T = L^2/D$ and $R = T/(1.41 \times C_L)$. Here, L is the diffusion length, D is the diffusion coefficient, and C_L is the limiting capacitance. By fitting, only T and R can be obtained.

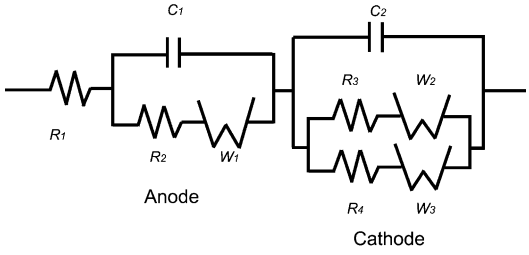

Fig. 1. Equivalent circuit used to fit the measured impedance of commercial Li-ion batteries. R_1, resistance of electrolyte and current collector; $R_{2–4}$, interfacial resistance; C, capacitance of electrode surface layer; $W_{1–3}$, Warburg impedance.

3. Results and discussion

3.1. Impedance depending on the state of charge

First of all, in order to assign individual components contributing to total impedance, the impedances of the batteries with various states of charge (SOC) were measured. Fig. 2 shows the Cole–Cole plot of the measured impedances at presented battery voltages and frequency ranges. Note that impedances at 4 or 3.8 mHz are indicated by arrows in the figure for comparison. It is seen that the total impedance increased with the decrease of the SOC. The impedances were fitted to the circuit shown in Fig. 1. Fig. 3(a) shows the fitted values of resistance. R_2 and the sum of R_3 and R_4 show a slight increase with the decrease of SOC. Here, the higher resistance is attributed to cathode resistance, and the lower is to anode [3–5,9]. R_1 was nearly constant for the voltage ranges used here.

From the fitted values of T appeared in Eq. (1), Li-ion diffusion coefficients (D) in both electrodes can be obtained by $D = L^2/T$ if the diffusion length is known. D in both $LiClO_4$ and carbon has been independently studied at

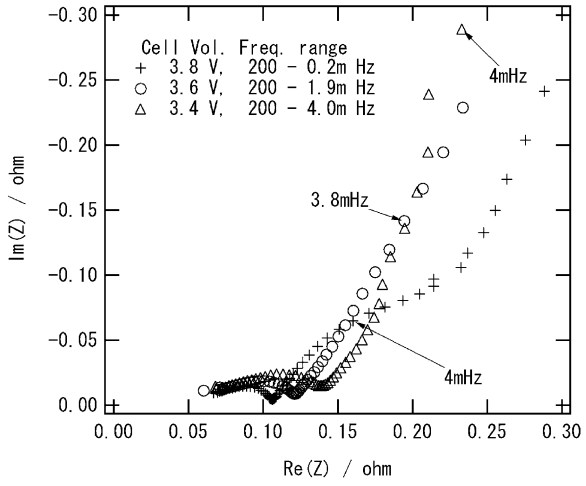

Fig. 2. Typical Cole–Cole plot of commercial Li-ion battery with several different cell voltages. The lowest frequencies measured here were different due to the large difference of impedance scale. Impedances at 4 or 3.8 mHz were also indicated by arrows.

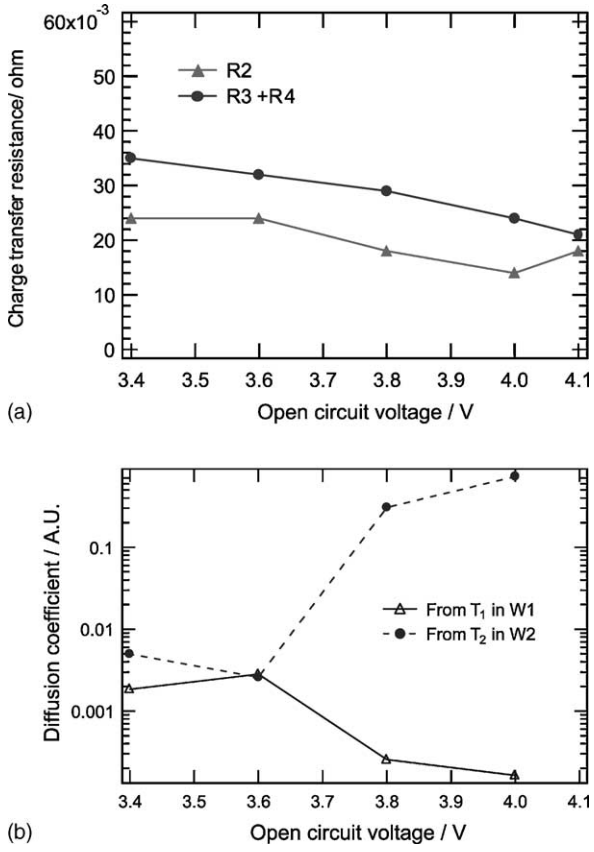

Fig. 3. Plots of the values obtained from the fits with the impedance in Fig. 2: (a) electrode–electrolyte interface resistance; (b) reciprocal of T appeared in Warburg impedance. Vertical axis of the plot (b) is labeled as diffusion coefficient, since the value of $1/T$ is proportionally related to Li-ion diffusion coefficients in active materials.

different SOCs. Here, we wish to compare the fitted results and previous reported values. Since the L is not clear here, instead of comparing values, we compare the dependence of D on SOC. Fig. 3(b) shows the reciprocal of the fitted value of T_1 and T_2, which appears in the Warburg impedances W_1 and W_2, respectively, in Fig. 1. The plot showed that the reciprocal of T_1 decreased and that of T_2 increased at high SOC. These trends of Li-ion diffusion coefficients are consistent with previous results [10] and other reports [12,13], if the W_2 is assigned to the cathode and the W_1 is the anode.

Using the fitted values of limiting capacitances for anode and cathode, the battery capacity at each open circuit voltage was estimated by summing both limiting capacitances. The result shown in Fig. 4 indicates that most of the capacity is at above 3.6 V and the capacity peak is at between 3.8 and 4.0 V. In order to compare the order of the results, chronoamperometry measurements were performed on the same battery by applying a 10 mV potential step from several voltages. The total amount of charge flowing from the battery was obtained by integrating the corresponding current transients. The obtained capacities were also plotted in Fig. 4, showing the comparable values obtained from the fits.

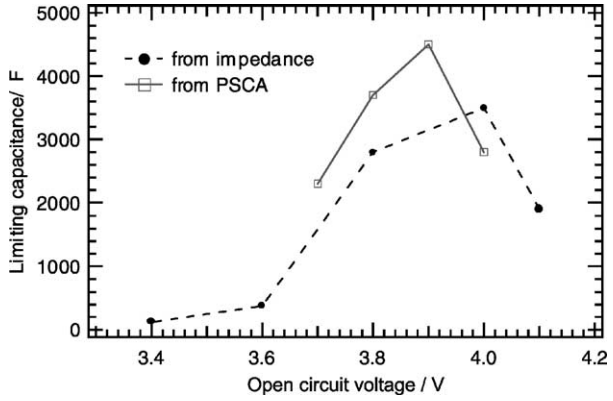

Fig. 4. Battery capacitances at difference cell voltages. Closed circles show the values obtained from the fits, and open squares were obtained from chronoamperometry measurements.

3.2. Influence of charge–discharge cycles

Fig. 5 shows the discharge capacity versus cycle number of the battery. The capacity decreased from about 580–450 mAh in 200 cycles. Fig. 6 shows the battery impedance between 200 Hz and 0.2 mHz at the cell voltage of 4.0 V, measured after the presented number of cycles. It can be seen that the imaginary value at very low frequency increased with the cycle number. The very low frequency impedance is related with the limiting capacitance, and hence the observations indicate that the amount of active materials is decreased, which could be caused by phase changes or dissolution.

The measured impedance was fitted to the equivalent circuit used above. The fitted values are plotted in Fig. 7, showing that the interfacial resistance of cathode increased with the cycle number, while that of the anode remained nearly constant. These results could be interpreted assuming that the anode is rather stable after the formation of a passive layer during the initial cycle, and the surface layer on the cathode would be growing due to the strong oxidizing power

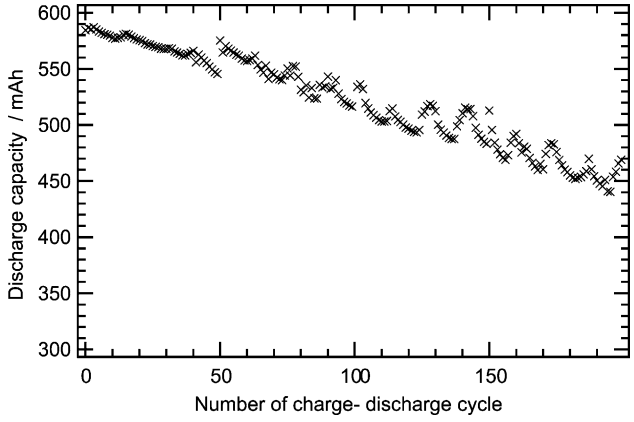

Fig. 5. Battery discharge capacity with the number of charge–discharge cycles.

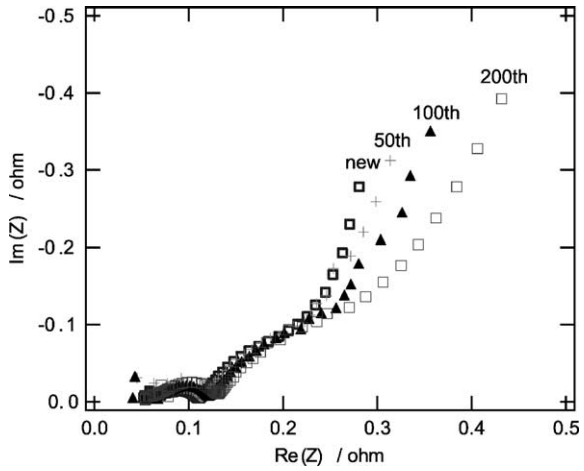

Fig. 6. Typical Cole–Cole plot of the battery at the cell voltage of 4.0 V. The measurements were repeated after the presented number of cycles. The frequency range was 200–0.2 mHz.

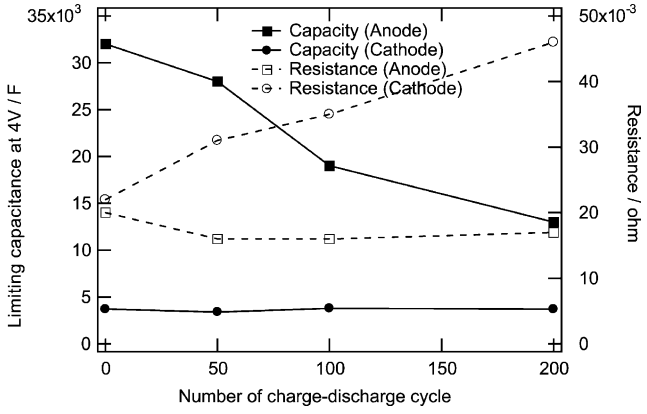

Fig. 7. Values obtained by the fits of the impedance shown in Fig. 6 with the number of cycles. Right axis shows the interface resistance and the left axis shows the limiting capacitance.

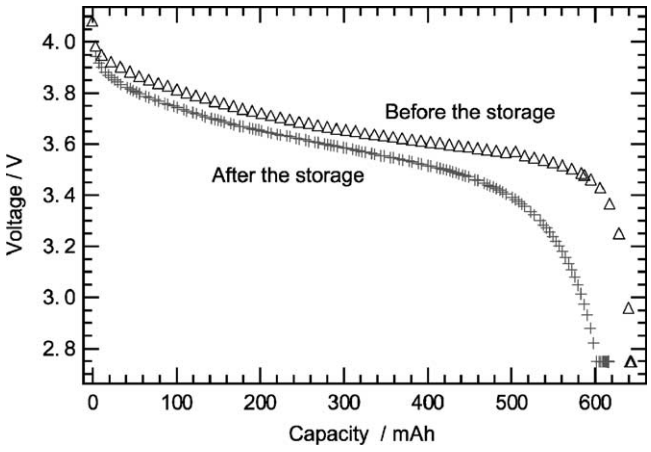

Fig. 8. Discharge profile of the battery at a 1 C rate before and after storage at 50 °C.

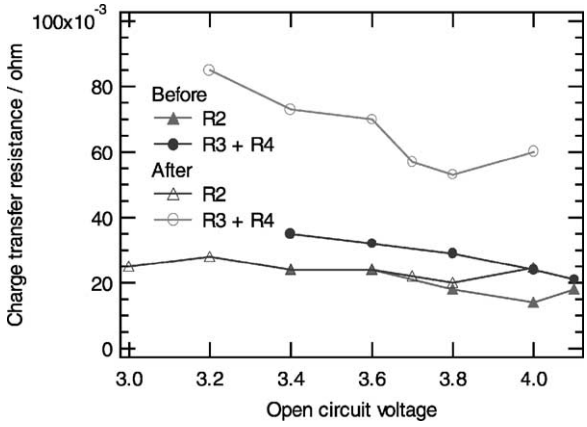

Fig. 9. Fitted values of interfacial resistances obtained from the battery impedance before and after storage.

of Co^{4+} in the charged state [3]. For the limiting capacitance, only that of the anode was decreased with the cycle number. Hence, the capacity fade was attributed to the increase of the cathode resistance and the decrease of anode capacitance. These results show the advantage of employing wide range frequency measurements on the impedance for the capacity fade studies.

3.3. Influence of high temperature storage

Fig. 8 shows the discharge curves of a battery at a 1 C rate before and after 20 days storage at 50 °C environment. The capacity was decreased about 25% if the cutoff voltage is set at 3.5 V. The impedance of the battery after storage was measured at various states of charge, and the fitted results were shown in Fig. 9. In this case, the capacity fade was partially attributed to the increase of the cathode interface resistance. The sum of the fitted values of the limiting capacitances decreased. However, a clear difference from each electrode contribution was not obtained at this moment.

4. Conclusions

The impedance of prismatic commercial Li-ion batteries was measured under various conditions. The impedance was fitted with a previously proposed equivalent circuit. The plots of the fitted values versus state of charge showed similar trends observed by other groups. Hence, fitting parameters were assigned to each electrode in the comparison. With the assignments, the impedance of the battery after cycling was analyzed, showing that the capacity fade was caused by an increase of cathode interfacial resistance and a decrease of anode capacity. The capacity fade due to high temperature storage of the battery appeared with the increase of cathode interfacial resistance on the equivalent circuit. These results indicate that two electrode

measurements of battery impedance for a wide range of frequencies can be interpreted with the equivalent circuit, providing an analysis tool for the study of capacity fading.

Acknowledgements

This work was supported in part by Grant-in-Aid for COE Research ''Molecular Nano-Engineering'' and the 21st Century COE Program 'Practical Nano-Chemistry' from the Ministry of Education, Culture, Sports, Science and Technology, Japan.

References

[1] P. Arora, R.E. White, M. Doyle, J. Electrochem. Soc. 145 (1998) 3647.
[2] J.-S. Kim, Y.-T. Park, J. Power Sources 91 (2000) 172.
[3] D. Zang, B.S. Haran, A. Durairajan, R.E. White, Y. Podrazhansky, B.N. Popov, J. Power Sources 91 (2000) 122.
[4] J. Baker, P. Shah, G. Nagasubramanian, D. Doughty, Electrochem. Soc. Proc. 99-25 (1999) 664.
[5] G. Nagasubramanian, J. Power Sources 87 (2000) 226.
[6] J. Li, E. Murphy, J. Winnick, P.A. Kohl, J. Power Sources 102 (2001) 294.
[7] Y. Saito, K. Takano, A. Negishi, K. Nozaki, K. Kato, Electrochem. Soc. Proc. 99-25 (1999) 671.
[8] T. Momma, K. Tsuchiya, T. Osaka, Abstracts of the 200th Electrochemical Society Meeting, 2001, 135 pp.
[9] T. Momma, K. Tsuchiya, T. Osaka, submitted for publication.
[10] T. Momma, K. Tsuchiya, T. Osaka, manuscript in preparation.
[11] T. Atsumi, Y. Nakata, K. Kobayakawa, K. Negishi, N. Yamazaki, Y. Sato, Electrochemistry 8 (2001) 603.
[12] T. Uchida, T. Itoh, Y. Morikawa, H. Ikuta, M. Wakihara, Denki Kagaku 12 (1993) 1390.
[13] H. Sato, D. Takahashi, T. Nishina, I. Uchida, J. Power Sources 68 (1997) 540.